Model and Field Testing of a Heavy-Duty Gas Turbine Combustor

Kook-Young Ahn*, Han-Seok Kim
Combustion & Environment Engineering Group,
Korea Institute of Machinery and Materials, 171, Jang-Dong, Yusung-Ku, Taejon 305-343, Korea
Vjacheslav Ivanovich Antonovsky
Turbine Institue, NPO CKTI, St. Petersburg, Politechnicheskaya Str. 24, Russia

The results of stand and field testing of a combustion chamber for a heavy-duty 150 MW gas turbine are discussed. The model represented one of 14 identical segments of a tubular multican combustor constructed 1:1 scale. The model experiments were executed at a lower pressure than that in a real gas turbine. Combustion efficiency, pressure loss factor, pattern factor, liner wall temperature, flame radiation, fluctuating pressure and NOx emission were measured at partial and full loads for both model and on-site testing. The comparison of these items in the stand and field test results led to has the development of a method of calculation and the improvement of gas turbine combustors.

Key Words : Model, Field Testing, Liner Wall Temperature, Combustion Efficiency, Pattern Factor, Pressure Loss Factor, Flame Radiation, NOx Emission, Comparison

1. Introduction

A model combustor testing is indispensable to develop a new heavy-duty gas turbine. In order to calculate the combustion characteristics of combustor, complicated physicochemical processes inside the combustor should be understood.

In a modern heavy-duty combustor, the air pressure reaches a few tens of atmospheres and the mass flowrates are on the order of 100 kg/s. In model testing, the pressure and air mass flowrate are essentially less than in real conditions of a heavy-duty gas turbine. Due to the lack of test facilities and operating expenses, model testing has been conducted instead of real one. Therefore, clear understanding of model and on-site correlation of combustor characteristics is desired.

---
* Corresponding Author,
  E-mail : kyahn@mailgw.kimm.re.kr
  TEL : +82-42-868-7324; **FAX** : +82-42-868-7284
  Combustion & Environment Engineering Group, Korea Institute of Machinery and Materials, 171, Jang-Dong, Yusung-Ku, Taejon 305-343, Korea.(Manuscript Received September 27, 2000; **Revised** May 10, 2001)

Combustor model testing was carried out on a special large-scale stand. The model combustor represented the final variant of the combustion chamber, which had been as a result of numerous experiments, provided with different liners, burners and atomizers, as well as dilution devices.

Some results of model and on-site experiments are presented in this paper. The comparison of paramerers such as the combustion efficiency, pressure loss factor, pattern factor, liner wall temperature, flame radiation, fluctuating pressure and NOx emission of model and real combustion chamber provides a useful design and calculation method of gas turbine combustors.

2. Combustion Chamber: Model and Field Test Program

The heavy duty gas turbine GTE-150 was designed based on a simple thermal circuit with one shaft turbogroup and was intended for both peak load and semi-peak load operation. According to this concept, the combustion chamber was constructed as a tubular (multican) type. Fourteen identical liners were placed in separate
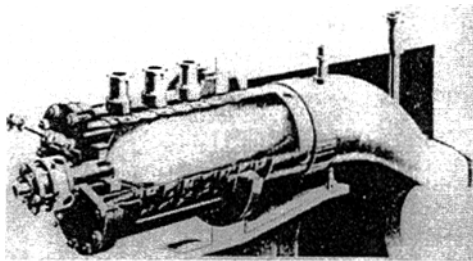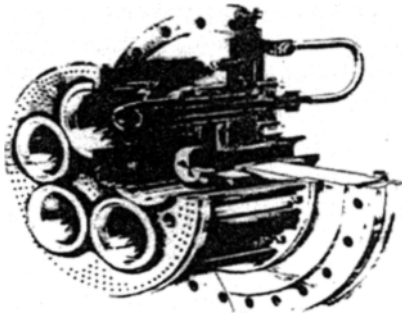
(a) Single-burner combustion section
(first stage of development)

(b) Multi-burner front device

Fig. 1   Combustion chamber of GTE-150

Fig. 2   Air-assist atomizer

sections, whose axes were parallel to the axis of the turbogroup. A section of the combustor is illustrated in Fig. 1(a). In addition to the liner, each section contains an atomizer, a vane swirler, a pressure casing, a burner device and a transition piece. Between sections, the connecting branch pipes are established, inside of which interconnectors are located. In this way the problem of pressure alignment between next sections, as well as the light-round problem was solved. The compressed air enters the volume of the connecting cylinder and is distributed between the sections of the combustor. About 25 % of the air enters the four dilution holes. The remainder of the air passes into the annular channels between casings and liners. On its way to the burner devices, the air is allocated to cooling and combustion holes. The high-speed jets of air leaving the combustion holes provide a rather productive fuel-air mixing that contributes to intensive burning of the fuel and makes possible the light-round of the sections. A vane air swirler with a vane outlet angle of 45° is used as a flame stabilizer. A transition piece connects the liner with the turbine vanes. The combustor of GTE-
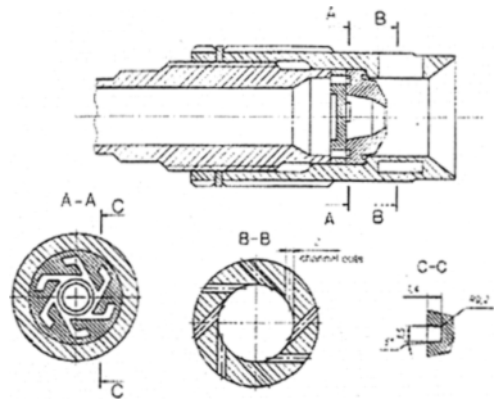
150 has a combustion loading rate of U_S=174.9 $W/m^2/Pa$. It is almost three times higher than the U_S of the combustion chamber for a previous Russian heavy-duty gas turbine GT-100-750 with a capacity of 100 MW.

In this paper, the results of testing of the combustion chamber with single burner device are presented. The results of a combustor with a five-burner device, as shown in Fig. 1(b), were published earlier (Antonovsky, 1990).

In the gas turbine GTE-150, air-assist atomizers were used. In these atomizers, a high quality atomization has been achieved. With a combination of pressure-swirl atomization and an additional fuel-drop splitting. Fuel drops are split immediately after the fuel nozzle due to the kinetic energy of the rotating high-speed air flow. The particulars of the applied air-assist atomizer can be found in Antonovsky (1991). The principal outline sketch of the atomizer is shown in Fig. 2. On the cross section A-A one can see fuel tangential ducts and a fuel swirl chamber. On the cross section B-B the atomizing air path is shown. In our atomizer, the ratio of atomizing air to fuel was in the range from 0.8 to 1.0. A special compressor with a pressure ratio of about 2 supplied air to the atomizer. The inlet of this auxiliary compressor was connected with the outlet of the main compressor. The use of air-assist atomizers has provided high quality fuel atomization and acceptable smoke level at the exit of the chimney.

Table 1 The design characteristics of the combustion chamber

Combustion product temperature at the exit of the combustor (the first stage of the GTE-150 mastering), t_{1T}, ℃	950
Combustor inlet air temperature t_A, ℃	372
Combustor inlet air pressure (inside the GT interconnecting cylinder) P_A, MPa	1.29
Air mass flow rate one section of the combustor A, kg/s	40.0
Fuel mass flow rate for one section of the combustor F, kg/h	2387
Combustion efficiency η, %	99
Pressure loss factor (within interconnecting cylinder transition piece exit) δP, %	5
Excess air coefficient a_Σ, -	4.23
Atomizing air mass flow rate for one section A_{aA}, kg/h	2387
Combustion loading Us, W/m²/Pa	174.9
Parameters of air at ignition for one section:	
Air mass flow rate A, kg/s	2.82
Air pressure P_A, MPa	0.116
Air temperature t_A, ℃	57
Excess air coefficient a_Σ, -	11.0

The combustion chamber was equipped with fuel supply and fuel injection systems. Liquid fuel with a caloric heat H=42.530 MJ/kg was used. Every can had its own igniter which used a propane-air mixture. The subsequent field tests showed that it was not necessary to install all 14 igniters, because the light-round system operated effectively.

The purpose of the model test program was to select the best version of the combustors, and then to establish the performance characteristics of the combustor. The performance parameters included combustion efficiency, temperature conditions of the metal, non-uniformity of turbine inlet temperature(the pattern factor), flame radiation, pressure losses, and concentration of harmful emissions in combustion products. After the model testing, field tests were conducted to conform the performance characteristics comparing with model test ones.

The design characteristics of the combustion chamber under discussion are shown in Table 1.

The following parameters were kept identical both the model and field combustor tests.

- Geometrical identity of combustors.
- The combustion product temperature at the exit of both combustors ($t_{1T}^N = t_{1T}^M$).

- The air temperatures entering combustion chambers ($t_A^N = t_A^M$).
- The velocity of air in similar apertures of the flame tubes ($W^N = W^M$).
- The same kind of fuel.
- The mean sizes of liquid fuel drops, as well as their distribution in the fuel spray-cone and their velocities.

Assuming that in both combustors the burning of fuel drops is accomplished before they reach dilution holes ($\eta^* > 0.99$), the rules listed above mean the combustion loading U_s [W/m²/Pa] in full-scale is same as the model one.
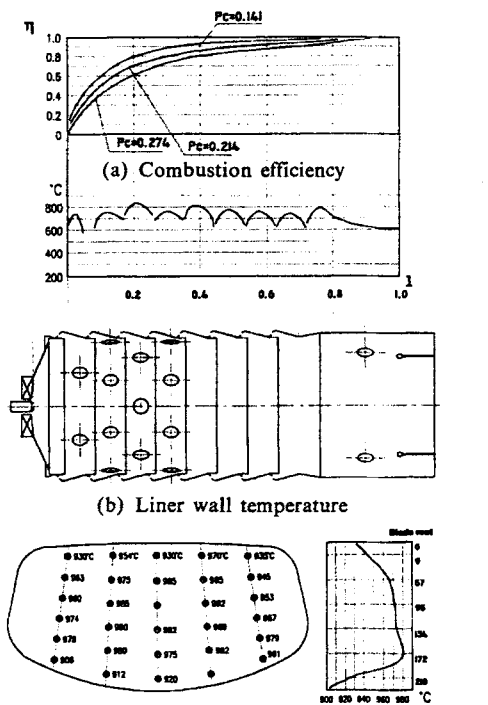
$$U_s^N = U_s^M = F^N H / S_L / P_A^N = F^M H / S_L / P_A^M.$$

Here the top indices N and M designate "natural" and "model" conditions; S_L is the cross section area of the liners.

Thus, the model test pressure P_A^M, fuel flowrate F^M and air flowrate A^M were lower than the corresponding values for the natural combustor.

$$F^M = (P_3^M / P_3^N) F^N; \quad A^M = (P_3^M / P_3^N) A^N.$$

The stand tests were performed on a model combustor which consisted of a casing, liner, burner device and a transition piece. The model section represented the bottom section of the onsite combustor.

(a) Combustion efficiency

(b) Liner wall temperature

(c) Distribution of combustion product temperature at the exit of the transition piece

Fig. 3 Results of stand tests; $U_S = 174.0W/(m^2Pa)$, $t_A = 370°C$, $t_{IT}^m = 962°C$.

3. Results of Model Testings

The combustion chamber had been ignited reliably. At the moment of ignition, the combustion product temperature peak, measured at the exit of the transition piece, had not exceeded 320°C. The character of fuel burning out is shown in Fig. 3(a). Increasing the pressure inside the combustor results in some retardation of burning in the primary zone of combustor. However the

fuel burning was accelerated at the downstream of liner and compensated its temporary braking in the beginning of the combustion process. In any case the completeness of liquid fuel combustion, η, within the liner length was not less than 99.0 %. The stability limits of combustion chamber were determined by a gradual reduction in the fuel flow rate utill the moment of a blowout. The flame blowout took place at an excess-air coefficient α_Σ of more than 17, corresponding to air heating of less than 130°C. The concentration of oxides of nitrogen (NOx) in combustion products had not exceeded 220 mg/m³ (hereinafter NOx are given for dry combustion products at 15% of O_2).

The liner wall temperature is shown in Fig. 3 (b). The nondimensional length of the liner, $1 = L/L^*$, is used in this figure. L is the distance between the atomizer and cross-section in question. L^* is the distance between the atomizer and dilution holes. We can see a typical distribution of liner wall temperature within the length of the separate drums, caused by air film-cooling of the drums and destruction of the jet boundary layer. The maximum temperature was located in the middle of the second drum (counting from the burner towards the transition piece) and amounted to 800 to 820°C. The maximum temperature of the transition piece is located near its exit on a generatrix. The absolute maximum temperature did not exceed 780°C.

The typical temperature distribution of combustion products at the exit of the transition piece is shown in Fig. 3(c). These data had been received in stand conditions with stationary multidot probes at 30 points. The maximum temperature, t_{1T}^{max}, was located at 2/3 of the channel height h, starting from the blade root. The relative non-uniformity of the temperature (the pattern factor)

$$100(t_{1T}^{max} - t_{1T})/(t_{1T} - t_A)$$

at full loading was 12 %.

The intensity of the thermal flame radiation J [kW/(m²sr)] was measured in several cross sections of the liner at various modes (Ahn and Antonovsky, 2001). The distribution of π J versus
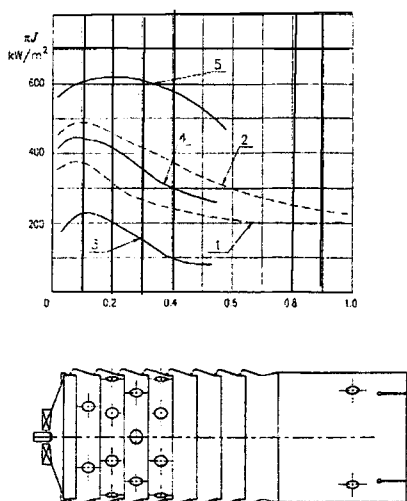
Before beginning field testing on a power plant, the segments No. 3 and No. 6 of the on-site combustor were equipped with the necessary devices and indicators for the implementation of the required measurements. In both the full-scale sections and the model combustor the following parameters were measured-the pressure of air and combustion products; flame radiation; combustor wall temperature; gas sampling.(Weeks, 1958 ; Saiton, 1990 ; Hayashi, 1996 ; Antonovsky, 1996).

Fig. 4 Thermal flame radiation:

1. Stand tests; U_S=136.0W/(m²Pa), t_A= 372℃, t_{iT}^m=950℃, P_C=0.141MPa
2. Stand tests; U_S=136.0W/(m²Pa), t_A= 369℃, t_{iT}^m=950℃, P_C=0.262MPa
3. Field tests; idle running
4. Field test; N_E=70MW
5. Field test; N_E=90MW

liner length is illustrated in Fig. 4, curves 1 and 2. The maximum thermal flame radiation was, in all cases, within the limits of the first two drums and could exceed 500 kW/m². The increasing of pressure in the combustion chamber always resulted in the increasing of thermal flame radiation. We guess the role of soot particles in the flame radiation.

The relative total (*-top index) pressure loss $100\Delta P^*/P_A$ measured at the connecting cylinder of the exit cross section of transition piece amounted to 5 %. Practically, in the connecting cylinder, P^*/P_A. The value of AT_A/P_A in model testing, proportional to air velocity in the liner holes, has to be equivalent to that in field testing one. The value in the stand tests is (AT_A/P_A)=40 ·645/1.29=20000 kgK/(sMPa). Note that the rather increased aerodynamic resistance of the combustion chamber under consideration requires better fuel-air mixing and higher value of combustion loading in the flame tube.

The measurements of fluctuating pressure had shown that the burning was stable at all modes;

the pressure oscillations appear to be broadband noise with frequencies of 60 to 80 Hz and 80 to 100 Hz. The average peak-to-peak amplitude of fluctuations did not exceed 4 to 5 kPa.

As we have already mentioned, the given results of the stand testing are of concern to the single-burner front device of the combustion chamber. The single-burner device was established on the basis of GTE-150 for the first stage of its development. A multi-burner front device, shown in Fig. 1(b), was further tested on the test rig. The experiments have shown, that in this case, the burning-out of fuel occurs more intensively and comes to an end on smaller length of the liner. The quality of the combustion chamber from the point of view of maximum metal temperature, the non-uniformity of the combustion product temperature after the transition piece and pressure fluctuations have not worsened. The concentration of nitric oxides has decreased a little. In the stand conditions it has amounted to 200 to 205 mg/m³. The details of stand testing of the multi burner combustor with temperature t_{iT}=1100℃ can be found in the previous paper (Antonovsky, 1990).

4. Field Tests Results: Comparison of Model and Field Tests

It is possible to ascertain a reliable ignition and a reliable light-round of the separate sections. At the moment of ignition, the burst of temperature of gases in front of the turbine (the hurl of the temperature), measured by low-inertia thermocouples, has not exceeded 380℃. At all modes of operation the combustion efficiency has been not less than 99 %. At a loading of 100 MW, the content of nitric oxides in combustion products sampled at the exit of the transition piece has achieved 340 mg/m³.

The combustion chamber operated quietly and steadily within the whole range of loading. The fluctuating pressure represented a broadband noise with frequencies 60 to 70 Hz and 80 to 100 Hz. The average double (peak-to-peak) amplitude of fluctuations did not exceed 5 to 6 Pa, and thus acceptable in Russia. At the moment of
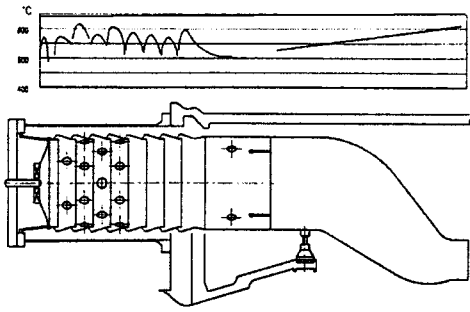
Fig. 5 Field tests, $N_E = 100MW$; liner wall and transition piece temperature

Fig. 6 Field tests, $N_E = 73.0MW$; Pressure loss of air and combustion product

ignition, idling and within the whole range of loading, the smoke emission did not exceed 3 to 4 SAE smoke number. At the chimney exit of the GTE-150, a slightly grayish the smoke appeared contrasting with the smoke of the neighboring chimney exit of GT-100. The moderate smoke emission of the GTE-150 exhaust gas was a consequence of application of the air-assist atomizers.

Enough items of information have been obtained concerning the liner wall temperature within the wide range of loading. A characteristic distribution of wall temperature versus liner length is shown in Fig. 5. It is similar to the liner wall temperature distribution of the model combustion chamber. Within the limits of every drum the maximum temperature is located on its middle. At the drum edges a rather low temperature is found. Such a distribution was caused by film cooling of the drum surface oriented to the flame. The maximum liner wall temperature of 830°C was found on the second drum. It was 20 to 30°C higher than maximum liner wall temperature of the model combustor under the same operating conditions. Also, Fig. 5 illustrates the temperature of the liner and transition piece. The maximum transition piece temperature of 820°C was located in its exit cross section on a generatrix. Similar result was obtained with the model testing, however the maximum temperature of the model combustor was lower by about 30°C.

In an earlier published paper (Weeks and Saunders, 1958) a rather significant role was found for the pressure in a combustor P_C on the

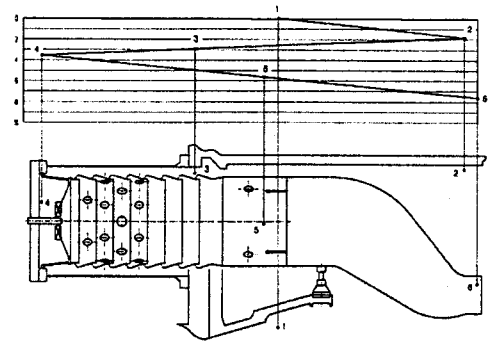flame emissivity ε_F and the effective temperature of flame radiation T_F. The present comparative research of model and full-scale combustors has confirmed the essential influence of P_C on ε_F and T_F. Really, the flame radiation intensity J measured within a zone of active fuel burning considerably exceeds the appropriate value of J measured in the model combustor as shown in Fig. 4. This circumstance is caused by the increase in the flame emissivity ε_F and the effective temperature of the flame radiation T_F at the transition from stand tests to field tests, since $P_C^N > P_C^M$. The value of ε_F increases due to the increase of media optical density. T_F increases due to the increase in the number of fuel-rich, high-temperature pockets. In these pockets the local temperature is close to the adiabatic flame temperature at the stoichiometric fuel/air ratio, $T_{a=1}$.

Pressure was measured in a number of points within the air and combustion products path. Thus, the absolute and relative pressure loss of the actual combustor as well as its elements were determined. Figure 6 shows the disposition of mea-suring points. Points 1 and 6 the measurements have been performed by total pressure probes (i. e. P_1^* and P_6^* have been measured), and at points 2, 3, 4 and 5 the static pressures P_2, P_3, P_4 and P_5 have been measured. The corrections on a dynamic pressure here were made.

It was found that the relative pressure loss of the total site mentioned, i. e. $100(P_1^* - P_6^*)/P_1^*$ or its separate sites $100(P_1^* - P_i^*)/P_1^*$, practically did not depend on loading. For the designed
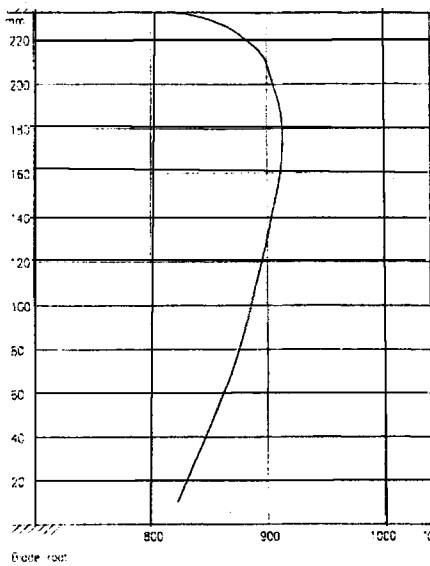
Fig. 7 Field tests, N_E=41.0MW ; radial distribution of combustion product temperature at the turbine inlet

single-burner combustion section, on the average, $100(P_1{}^*-P_6{}^*)/P_1{}^*$=7.49 %. There are two reasons for the larger pressure loss in the full-scale combustion chamber. First, in the full-scale combustor the value of AT_A/P_A is other than it should be from the design parameters of air on the combustor entrance. In field-tests the value of AT_A/P_A was not less than 2100 kgK/(sMPa). Secondly, at the stand conditions the pressure at point 1 (see Fig. 6), at the exit of the axial compressor, was not measured. Therefore only the pressure loss in the actual combustion chamber ($100(P_2{}^*-P_6{}^*)/P_2{}^*$) was determined to be less than $100(P_1{}^*-P_6{}^*)/P_1{}^*$.

Analysis of the pressure loss data also shows that about one quarter of the total pressure loss was in the transition piece. The over estimated pressure loss was caused, in particular, by the non-uniform speed and non-uniform temperature of combustion products at the entrance of the transition piece. At the same value of the AT_A/P_A, the pressure losses within the sites 2-5 of model and full-scale combustors were identical.

A typical combustion product temperature distribution in the radial direction, obtained by a traversing probe near the exit of the transition

piece, can be seen in Fig. 7. The maximum temperature was located at 2/3 of the channel height from the blade root. The identical radial distribution of temperature t_{1T} had been obtained in model testing. Irrespective of loading of the gas turbine it was found that

$$100(t_1{}^{max}-t_{1T})/(t_{1T}-t_A)=8.8 \text{ to } 12.0 \text{ %}.$$

This was recognized as a satisfactory characteristic. The value of this characteristic coincided with that obtained earlier with model testing.

The circuit gas temperature non-uniformity at gas turbine entrance (the pattern factor) is by no means the important gas turbine characteristic. With our model testing, this kind of characteristic could not be obtained. It is completely clear that the circuit non-uniformity of the gas temperature is determined by the non-uniformity of the fuel and air distribution among separate sections of the combustion chamber. Experience and theory convince us that the fuel distribution is more difficult than the air distribution, because of the different height location of atomizers and very small through passage areas of its fuel channels. Leading gas turbine firms have overcome these difficulties by installating volumetric fuel batchers, which distribute fuel among sections independent of the difference in the height location of atomizers and through passage areas of fuel channels. The fuel batchers were not installed on GTE-150. The uniformity of fuel distribution was achieved by a selection of atomizers with various flow rate characteristics.

The circuit gas temperature non-uniformity at turbine entrance has been obtained by measurement of combustion product temperatures with thermocouples. In every transition piece the thermocouple was located at 2/3 of the channel height measured from the blade root. This temperature was designated as $t_{C.P}$. A typical distribution of circuit temperatures is shown in Fig. 8. We can ascertain that the temperature distribution is not uniform. Some characteristics were used to describe the circuit temperature non-uniformity as in the above radial non-uniformity case. We define $t_{C.P}{}^{Max}$ as the value of maximal temperature measured, and $t_{C.P}{}^m$ as the mass mean temperature
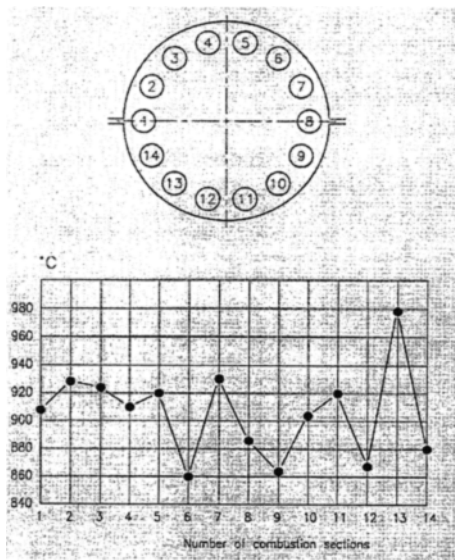
Fig. 8 Field tests, N_E=90.0MW ; circle distribution of the combustion product temperature at the turbine entrance

of combustion products at the turbine entrance. According to measurements and calculations, the difference in temperatures $(t_{C.P}{}^{Max} - t_{C.P}{}^m)$ in the range of loading of 60 to 90 MW amounts to 90℃, having a weak tendency to increase in the process of loading growth. The characteristics, 100 $(t_{C.P}{}^{Max} - t_{C.P}{}^m)/(t_{C.P}{}^m - t_A)$, was equal to 10 to 15 % and did not appear to have a predictable travel in the process of loading growth.

5. Conclusion

From the model and field testing of the combustion chambers, the following conclusions can be drawn.

(1) The relative aerodynamic pressure loss in similar locations of model and on-site combustors are identical.

(2) The position of the gas temperature maximum $t_{1T}{}^{max}$ in the radial direction in model and on-site combustors are identical.

(3) The characteristics of the radial temperature non-uniformity at the turbine entrance, 100 $(t_{1T}{}^{max} - t_{1T}{}^m)/(t_{1T}{}^m - t_A)$, is in the onsite combustor higher by 2 to 3 %. This can be explained by delayed burning in the on-site combustor in

which the pressure was much higher than that in the model conditions.

(4) Emissions of nitric oxides were higher in the on-site combustor than in the model combustor. The well known and accepted relationship can be used.

$$(NO_x)^N = (NO_x)^M (P_c^N / P_c^N)^n,$$

Where the exponent n is a constant and has a value of 0.30.

(5) The position of maximum liner wall temperature as well as temperature distribution on the liner length are identical in both combustors. The position of maximum liner wall temperature was on the middle of the second drum, counting from the burner. The values of the liner wall and the transition piece temperature in the on-site combustor were higher by 20 to 30℃ when compared to those of the model combustor.

References

Ahn, Kook-Young and Antonovsky, V. I., 2001, "Experimental Analysis of Radiative Heat Interchanges on Furnace Exit Plane of a Steam Boiler," *KSME International Journal*, Vol. 15, No. 2, pp. 239~247.

Antonovsky, V., Akoulov, V. and Shvedkov, V., 1990, "Some Results of Stand Testing of the GTE-150 Combustor at Mean Mass Gas Temperature at the Turbine Entrance 1100℃," CKTI Papers, Vol. 261, pp. 151~156.

Antonovsky, V., Akoulov, V., Shvedkov, V. and Lesnjak, O, 1991, "Investigation of GTE 150 at Application of Air-Assist and Airblast Atomizers," CKTI Papers, Vol. 266, pp. 49~56.

Antonovsky, V., 1996, "Thermal Radiation of Flame in Gas Turbine Combustion Chambers," *Proceedings of the Third International Symposium on Experimental and Computational Aerothermodynamics of Internal Flows*, September 16, Word Publishing Corporation, pp. 970 ~972.

Hayashi, S., Yamada, H. and Shimodaira, K., 1996, "Engine Testing of a Natural Gas-fired, Low NOx, Variable Geometry Combustor for a Small Gas Turbine," the *International Gas Tur-*

bine and Aeroengine Congress and Exhibition, UK, June 10-13.

Saiton, Y. and Fujimori, T., 1990, "Study of the Effects of Atomization Characteristics on NOx Emission for Airblast Atomizer with Premixed/ Prevaporized Tube (TS-67)," *Proceedings of the*

International Gas Turbine Congress 1999 Kobe, Vol. II, pp. 753~758.

Weeks, D. J. and Saunders, O. A., 1958, "Some Studies of Radiating Flames in a Small Gas Turbine Type Combustion Chamber," *J. Inst. Fuel*, Vol. 31, N 209, pp. 247~258.